Mathematical Problems in Engineering
Volume 4, pp. 115-133
Reprints available directly from the publisher
Photocopying permitted by license only

On a Numerical Model for Diffusion-Controlled Growth and Dissolution of Spherical Precipitates

R. VAN KEER[a] and J. KAČUR[b]

[a]*Department of Mathematical Analysis, Faculty of Engineering, University of Ghent, Galglaan 2, 9000 Gent, Belgium.* [b]*Institute of Numerical Analysis and Optimalization, Comenius University, Mlynská Dolina, 842 15 Bratislava, Slovak Republic.*

(Received 18 October, 1996)

This paper deals with a numerical model for the kinetics of some diffusion-limited phase transformations. For the growth and dissolution processes in 3D we consider a single spherical precipitate at a constant and uniform concentration, centered in a *finite* spherical cell of a matrix, at the boundary of which there is no mass transfer, see also Asthana and Pabi [1] and Caers [2].

The governing equations are the diffusion equation (2nd Fick's law) for the concentration of dissolved element in the matrix, with a known value at the precipitate-matrix interface, and the flux balans (1st Fick's law) at this interface. The numerical method, outlined for this free boundary value problem (FBP), is based upon a fixed domain transformation and a suitably adapted nonconforming finite element technique for the space discretization. The algorithm can be implemented on a PC. By numerous experiments the method is shown to give accurate numerical results.

Keywords: Diffusion kinetics; spherical precipitates; moving boundaries; finite elements

Classification Categories: 35K99, 76T05, 65N30

1 INTRODUCTION

Aaron *et al.* [3] dealed with a mathematical model for the diffusion-controlled growth and dissolution of precipitates in an homogeneous matrix. In that model, one single precipitate, taken to be spherical and at a constant, uniform concentration c_P, is placed in an *infinite* matrix. The problem consists of evaluating the time evolution of the precipitate-matrix

interface, coupled to the one of the radial symmetric concentration of dissolved element in the matrix. Here, the concentration at the interface has a fixed, known value c_I, characteristic for the temperature at which the growth and dissolution process takes place. Moreover, initially the matrix is uniformly at a concentration c_M and c_M is kept as the concentration of dissolved element at any time $t > 0$ at infinitely large distance of the precipitate, i.e. outside its influence. The expected concentration profiles are sketched in Fig 1 below. Here, notice the different position of c_I in the two cases.

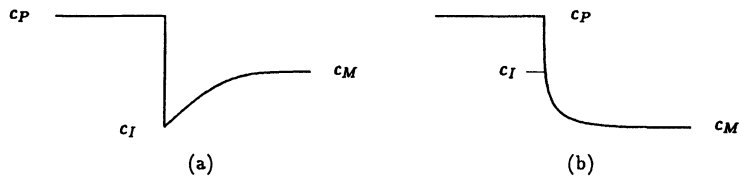

FIGURE 1 Concentration profiles: (a) precipitate growth, (b) precipitate dissolution

The governing equations are the diffusion equation for the dissolved element in the matrix and the flux balans at the interface. For the case of precipitate growth the analytical solution of this free boundary problem (FBP) has been constructed in [3].

Caers [2] refined this model in that the matrix is taken to be a *finite* sphere, in the centre of which is placed the spherical precipitate, see also [1]. The underlying assumption is that the matrix consists of identical cubic cells, in the centre of which is placed one single particle. In this way the overall process of growth and dissolution is reduced to the process in one basic cell, however with the drawback that the radial symmetry of the problem is lost. This drawback has been remedied by the introduction of *spherical* cells with the same volume as the cubic ones, so that the ratio of the mass in the precipitated phase and the mass in the dissolved phase remains the same. In this structure there is no mass transfer between neighbouring cells. The fact that the size of the precipitates is small compared to the diffusion distances, supports the assumption of spherical symmetrical concentration profiles around the particles.

For this FBP, stated in a precise form below (Section 2), no analytical solution exists. We present a fairly general and effective numerical method. We begin with a fixed domain transformation, resulting in a highly nonlinear, *nonlocal* initial boundary value problem (IBVP) for a

parabolic PDE, coupled with a 1st order ODE with respect to time (Section 3). We then derive a variational formulation of this problem. Next, we apply a *nonconforming* finite element approximation to the variational problem, using linear shape functions on a non uniform finite element mesh (Section 4). The nodes are distributed more densily near the end point of the space interval that corresponds to the moving matrix-precipitate interface. Moreover, near this end point the concentration profile is approximated by a quadratic polynomial in order to properly take into account the flux balance at the interface, cf. Liu *et al.* [4]. The semi-discrete problem can be simplified considerably by using a standard numerical quadrature rule, which is exact for polynomials of 1st degree and which, in particular, implies the lumping of the mass matrix. We are left with a strongly nonlinear initial value problem (IVP) for a system of 1st order ODEs with respect to time, the integration of which is done with a step-controlled Runge Kutta code, available e.g. from Mathematica 2.2.

The reliability of the fully discrete method, which can be implemented on a PC, has been confirmed in two manners (Section 5). First, during a certain time interval $[0, t_e]$, the length of which depends on a parameter of the kinetics of the process, the results for the precipitate growth are in very good agreement with those obtained in [3] for a large scale of kinetics parameters, even when a coarse mesh or when numerical quadrature is used. The results in [3], based upon analytical formulae, ought to be valid in $[0, t_e]$, during which the influence of the finite boundary of the matrix cell on the growth process is negligible. Secondly, still in the case of precipitate growth, for large values of time the numerical value of the precipitate radius must tend to the value of the particle radius in the steady state regime, being known exactly from a mass balance argument. A similar property must hold in the case of precipitate dissolution up to a nonzero limit particle radius. Also here we have obtained very good agreement between the numerical results and the exact ones.

As a secondary test of the numerical method, we also considered the case of precipitate dissolution with complete particle extinction. The calculated value of the finite extinction time T_e is not affected by the use of numerical quadrature for the construction of the finite element matrices. Moreover, the calculated values of T_e are in relative good agreement with results in [3] and [1], obtained by stationary interface models for particular sets of data.

2 MATHEMATICAL MODEL

A spherical precipitate with unknown, time varying radius $R(t)$ is centered in a spherical cell with radius L of an homogeneous matrix, cf. Fig. 2. The precipitate is taken to be uniformly at a constant concentration c_p, while the concentration profile $c(r, t)$, $R(t) < r < L$, of the dissolved element in the matrix is at any time $t > 0$ governed by Fick's 2nd law, the concentration at the matrix-precipitate interface $r = R(t)$ having a known constant value c_I. The position of the interface is related to this concentration profile.

When during a time interval $(t, t + \delta t)$ the radius of the precipitate changes from $R(t)$ to $R(t) + \delta R$, the mass balance reads

$$4\pi \cdot R^2 \cdot D \cdot \left.\frac{\partial c}{\partial r}\right|_{r=R(t)} \cdot \delta t = \frac{4}{3} \cdot \pi \cdot [(R+\delta R)^3 - R^3] \cdot (c_p - c_I).$$

Here $D \cdot \left.\frac{\partial c}{\partial r}\right|_{r=R(t)}$ gives the mass flux per unit time interval and per unit area from the matrix towards the surface of the precipitate (growth) or vice versa (dissolution), D being the diffusion coefficient.

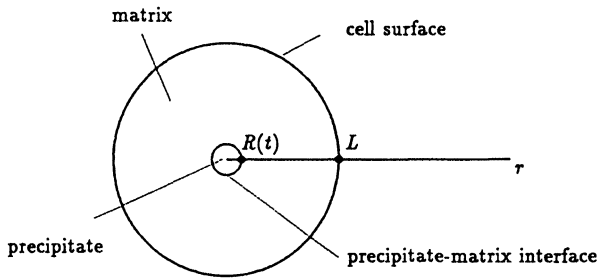

FIGURE 2 A spherical precipitate in a spherical cell of a matrix

The resulting FBP for the couple $[R, c]$ consists of

(a) the diffusion equation for the dissolved element in the matrix,

$$\frac{\partial c}{\partial t} = D \cdot \left(\frac{\partial^2 c}{\partial r^2} + \frac{2}{r} \cdot \frac{\partial c}{\partial r}\right) \quad (\equiv D \cdot \Delta c), \quad R(t) < r < L, \quad t > 0; \tag{2.1}$$

(b) a general linear flux condition at the cell surface,

$$-D \cdot \frac{\partial c}{\partial r} = b \cdot (c - \varphi), \quad r = L, \quad t > 0; \tag{2.2}$$

(c) two interface conditions,

$$c = c_I, \quad r = R(t), t > 0, \tag{2.3}$$

$$D \cdot \frac{\partial c}{\partial r} = (c_p - c_I) \cdot \frac{dR}{dt}, \quad r = R(t), t > 0; \tag{2.4}$$

(d) given initial data,

$$R(0) = R_0, \quad c(r,0) = c_0(r),\ R_0 < r < L. \tag{2.5}$$

In the physical problem considered in Section 1 there is no mass transfer at the cell surface, i.e. $b = 0$ in (2.2). We still retain (2.2) in its present form for the sake of generality. Condition (2.4) is implied by the mass balance mentioned above in the limit $\delta t \to 0$, $\delta R \to 0$. In the present FBP the data D, c_I, b and φ are given (positive) constants. However, the analysis below equally applies to the case of time dependent data. Moreover (2.1) may contain a reaction source term $F(c)$.

In Aaron *et al.* [3] an analytical solution to the FBP (2.1)-(2.5) has been derived for the case of precipitate growth, with $R_0 = 0$, $c_0(r) = c_M$ (constant) $> c_I$ *and* $L = \infty$, (2.2) being replaced by the limit condition $c(+\infty, t) = c_M$, for all $t > 0$. For the corresponding case of precipitate dissolution (now $c_M < c_I$, cf. Fig. 1) no analytical solution exists. For the FBPs with $L \neq \infty$ one has to ressort to a *numerical* approximation method, even for the case of precipitate growth, even when $R_0 = 0$, $c_0(r) = c_M$ and $b = 0$.

The first step towards a fully discrete method, outlined in this paper, is the reduction of (2.1)-(2.5) to a fixed domain IBVP and the variational formulation of this latter problem.

3 TRANSFORMATION TO A FIXED DOMAIN PROBLEM. VARIATIONAL FORMULATION

To remove the term $\frac{2}{r} \cdot \frac{\partial c}{\partial r}$ in (2.1) we first pass to the new unknown U,

$$U(r,t) = r \cdot c(r,t). \tag{3.1}$$

Next, by introducing the new variables

$$x = \frac{L - r}{L - R(t)}, \quad u(x,t) = U(r,t), \tag{3.2}$$

and by putting

$$z(t) = L - R(t), \tag{3.3}$$

the FBP (2.1)-(2.5) is transformed to a fixed domain IBVP for the couple existing of $u(x, t)$, $0 < x < 1$, $t > 0$ and $z(t)$, $t > 0$. The problem consists of

(a) the nonlinear, *nonlocal* parabolic PDE

$$\partial_t u = \frac{D}{z^2} \cdot \partial_x^2 u + \frac{x}{\alpha \cdot z^2 \cdot (L-z)} \cdot (\partial_x u(1,t) + z \cdot c_I) \cdot \partial_x u, \; 0 < x < 1, \; t > 0; \tag{3.4}$$

(b) the nonlinear ODE

$$\frac{dz}{dt} = \frac{1}{\alpha \cdot (L-z) \cdot z} \cdot (\partial_x u(1,t) + z \cdot c_I), \quad t > 0; \tag{3.5}$$

(c) the two BCs

$$-\frac{D}{Lz} \cdot \partial_x u + (\frac{b}{L} - \frac{D}{L^2}) \cdot u = b \cdot \varphi, \quad x = 0, \; t > 0, \tag{3.6}$$

$$u = c_I \cdot (L - z), \quad x = 1, t > 0; \tag{3.7}$$

(d) the two ICs

$$u(x,0) = u_0(x) \equiv (L \cdot (1-x) + R_0 \cdot x) \cdot c_0(L \cdot (1-x) + R_0 \cdot x), \; 0 < x < 1, \tag{3.8}$$

$$z(0) = L - R_0; \tag{3.9}$$

where

$$\alpha = \frac{(c_p - c_I)}{D}.$$

The *nonlocal* character of (3.4) is reflected in the appearing partial derivative $\partial_x u(1, t)$ of the unknown taken at $x = 1$; see also (3.5).

Moreover, by introducing the new unknown

$$w = u - c_I \cdot (L - z), \quad 0 < x < 1, t > 0, \tag{3.10}$$

we are left with a similar IBVP for the couple existing of $w(x, t)$, $0 < x < 1$, $t > 0$, and $z(t)$, $t > 0$, now with an homogeneous Dirichlet BC at $x = 1$.

This last problem can be given a variational formulation. We introduce the function spaces

$$V = \{v \in H^1(0,1) \mid v(1) = 0\}, \quad W = \{v \in H^2(0,1) \mid v(1) = 0\},$$

as the space of test and trial functions respectively. Here $H^1(0, 1)$ and $H^2(0, 1)$ are the usual first and second order Sobolev spaces on the interval $]0,1[$.

Dealing with the parabolic PDE for $w(x, t)$ in the usual way, we arrive at the following variational problem:

Find the couple of the smooth function $z(t)$, $t > 0$, and the function $w(.,t)$, $t > 0$, with $w \in W$ and $\partial_t w \in L_2(0, 1)$ for every $t > 0$, which obey the nonlinear integral identity

$$(\partial_t w, v) = -\frac{D}{z^2} \cdot (\partial_x w, \partial_x v) + \frac{(\partial_x w(1,t) + z \cdot c_I)}{\alpha \cdot (L - z) \cdot z^2} \cdot [(x \cdot \partial_x w, v) + z \cdot c_I \cdot (1, v)]$$

$$+ \frac{D}{z} \cdot \left[\left(\frac{1}{L} - \frac{b}{D}\right) \cdot w(0,t) + c_I \cdot \left(\frac{1}{L} - \frac{b}{D}\right) \cdot (L - z) + L \cdot \frac{b}{D} \cdot \varphi \right] \cdot v(0),$$

for all $v \in V$ and for (almost) every $t > 0$, (3.11)

coupled with the analogue of (3.5), viz

$$\frac{dz}{dt} = \frac{1}{\alpha \cdot (L - z) \cdot z} \cdot (\partial_x w(1,t) + z \cdot c_I), \quad t > 0, \tag{3.12}$$

under the ICs

$$w(x,0) = u_0(x) - c_I \cdot (L - z(0)), \quad 0 < x < 1, \quad z(0) = L - R_0, \tag{3.13}$$

where $u_0(x)$ is given by (3.8).

In (3.11), (.,.) stands for the inner product in $L_2(0, 1)$. Notice the appearance of $\partial_x w(1, t)$ in the variational equation (3.11), both directly and through the function z, see (3.12). Due to the continuous embedding of the space $H^2(0, 1)$ in the space $C^1([0, 1])$ of smooth functions on the closed interval $[0, 1]$, $\partial_x w(1, t)$ is well defined.

The existence of a solution to this type of IBVP is discussed in Pani [5]. The second step towards a numerical method for the original FBP (2.1)-(2.5) is the approximation of the couple $[w(x, t), z(t)]$, $0 < x < 1$, $t > 0$, by a suitable finite element method with respect to x at any $t > 0$.

4 NONCONFORMING FINITE ELEMENT APPROXIMATION

Let $0 = x_1 < x_2 < \ldots < x_N < x_{N+1} = 1$ be a partition of the interval $[0, 1]$, where $N \in \mathrm{N}_0$ is given. Denote $h_i = x_{i+1} - x_i$, $1 \le i \le N$. We use a *nonuniform* partition of $[0, 1]$ defined by

$$h_i = \frac{2}{N+1} \cdot \frac{N - i + 1}{N}, \quad 1 \le i \le N.$$

Thus the FE-mesh is gradually refined from the begin point $x = 0$ to the end point $x = 1$, these points corresponding, respectively, to the cell-surface $r = L$ and to the precipitate-matrix interface $r = R(t)$ in the original FBP (2.1)-(2.5).

Introduce the standard finite dimensional subspaces of $C^0([0, 1])$

$$X_h = \{v \in C^0([0,1]) | v \text{ is a first order polynomial in }]x_i, x_{i+1}[, 1 \leq i \leq N\} \quad (4.1)$$

and

$$V_h = \{v \in X_h \mid v(1) = 0\}. \quad (4.2)$$

Clearly, $V_h \subset V$, but $V_h \not\subset W$. Thus, when besides V also W is approximated by the space V_h in (3.11), the corresponding FEM is *nonconforming* in the terminology of e.g. Carey and Oden [6]. For the sake of computational elegance, this choice of FEM is made below. However we improve the approximation of the derivative $\partial_x w(1, t)$, the appearance of which in (3.11) required passing to a subspace W of $H^2(0,1)$ as the space of trial functions.

(The simplest choice of a conforming FEM requires cubic Hermite finite elements to approximate w, see e.g. [6], which is computationally cumbersome.)

Let $(\varphi_i)_{1 \leq i \leq N}$ be the canonical basis of V_h, i.e. $\varphi_i \in X_h$ and $\varphi_i(x_j) = \delta_{ij}$, $1 \leq i \leq N$, $1 \leq j \leq N + 1$.

As an approximation of the couple $[w, z]$, obeying (3.11)-(3.13), we define the couple $[w_h, z_h]$, with

$$w_h(x,t) = \sum_{i=1}^{N} \xi_i(t) \cdot \varphi_i(x), \quad 0 < x < 1, \quad t > 0, \quad (4.3)$$

by a system similar to (3.11)-(3.13). Here, in the analogue of (3.11) the test function v is restricted to V_h, of course. Moreover we *don't* substitute $\partial_x w(1, t)$ by $-\dfrac{\xi N(t)}{h_N}$, which would be in agreement with (4.3), but we put, cf. Fig. 3,

$$\partial_x w(1,t) \approx m(\xi_{N-1}(t), \xi_N(t)) \quad (4.4)$$

$$\equiv \frac{h_N}{h_{N-1} \cdot (h_{N-1} + h_N)} \cdot \xi_{N-1}(t) - \frac{h_{N-1} + h_N}{h_{N-1} \cdot h_N} \cdot \xi_N(t)$$

The choice of a suitable approximation of $\partial_x w(1, t)$ is essential for the accuracy of the algorithm, as this derivative arises from the flux balans condition (2.4) in the original FBP and will lead to the velocity $\dfrac{dR}{dt}$ of the

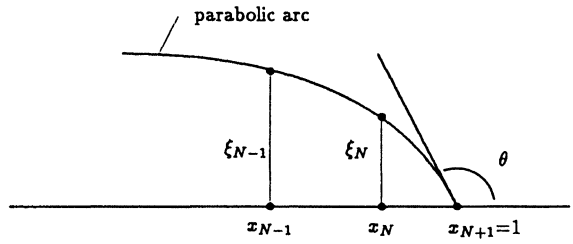

FIGURE 3 Finite element approximation of $\partial_x w(1, t)$ by $tg\theta$

precipitate-matrix interface, through (3.3) and (3.12). The expression (4.4) results from the *parabolic* arc which is shown in Fig. 3 and which is taken to approximate $w(x,t)$ near $x = 1$, cf. Liu *et al.* [4].

Denoting

$$C(t) = [\xi_1(t), \dots, \xi_N(t)]^T, \quad t > 0,$$

the resulting IVP for $C(t)$ and $z_h(t)$, $t > 0$, reads:

Solve the system of N+1 nonlinear 1st order ODEs

$$M \cdot \frac{dC}{dt} = -\frac{D}{z_h^2} \cdot Q \cdot C + \frac{m(\xi_{N-1}, \xi_N) + z_h \cdot c_I}{\alpha \cdot (L - z_h) \cdot z_h^2} \cdot [R \cdot C + z_h \cdot c_I \cdot E]$$

$$+ \frac{D}{z_h} \cdot \left[\left(\frac{1}{L} - \frac{b}{D}\right) \cdot \xi_1 + c_I \cdot \left(\frac{1}{L} - \frac{b}{D}\right) \cdot (L - z_h) + L \cdot \frac{b}{D} \cdot \varphi \right] \cdot e_1, \; t > 0, \quad (4.5)$$

$$\frac{dz_h}{dt} = \frac{m(\xi_{N-1}, \xi_N) + z_h \cdot c_I}{\alpha \cdot (L - z_h) \cdot z_h}, \; t > 0,$$

under the ICs

$$C(0) = M^{-1} \cdot P \quad , \quad z_h(0) = L - R_0. \quad (4.6)$$

Here, E, e_1 and P are $(N \times 1)$-matrices, defined as follows

$$E = [E_1, E_2, \dots, E_N]^T, \quad E_i = \int_0^1 \varphi_i(x)dx, \quad 1 \le i \le N, \quad (4.7)$$

$$e_1 = [1, 0, \dots, 0]^T,$$

$$P = [p_1, p_2, \dots, p_N]^T,$$

where

$$p_i = \int_0^1 [(L \cdot (1-x) + R_0 \cdot x) \cdot c_0 (L \cdot (1-x) + R_0 \cdot x) - c_I \cdot R_0] \cdot \varphi_i(x)dx, \; 1 \le i \le N.$$

Furthermore, the matrices M (mass matrix), Q (stiffness matrix), and R, entering (4.5)-(4.6), are $(N \times N)$-matrices, defined by

$$M = (M_{ij})_{1\le i,j\le N}, \quad M_{ij} = \int_0^1 \varphi_j(x)\varphi_i(x)dx,$$

$$Q = (Q_{ij})_{1\le i,j\le N}, \quad Q_{ij} = \int_0^1 \varphi_j'(x)\varphi_i'(x)dx, \tag{4.8}$$

$$R = (R_{ij})_{1\le i.j\le N}, \quad R_{ij} = \int_0^1 x\varphi_j'(x)\varphi_i(x)dx.$$

We recall that M, Q and R are tri-diagonal matrices. They explicitly read, in a shorthand notation, (with the nonzero elements on each row listed from left to right),

$$M = \frac{1}{3}\left[\frac{h_{i-1}}{2}, h_{i-1}+h_i, \frac{h_i}{2}\right]_{1\le i\le N}, \quad (h_0 = 0),$$

$$Q = \left[-\frac{1}{h_{i-1}}, \frac{1}{h_{i-1}}+\frac{1}{h_i}, -\frac{1}{h_i}\right]_{1\le i\le N}, \quad (\frac{1}{h_0} = 0), \tag{4.9}$$

$$R = -\left[\frac{x_{i-1}}{2}+\frac{h_{i-1}}{3}, \frac{h_{i-1}+h_i}{2}, -\frac{x_{i+1}}{2}+\frac{h_i}{3}\right]_{1\le i\le N}, \quad (x_0 = h_0 = 0).$$

In this notation it is tacitly understood that on the 1st and Nth row there is only one nonzero off-diagonal element and that for $i = 1$ the meaningless terms are put equal to zero (as indicated). The column matrix E, (4.7), is

$$E = \left[\frac{h_1}{2}, \frac{h_1+h_2}{2}, \ldots, \frac{h_{i-1}+h_i}{2}, \ldots, \frac{h_{N-1}+h_N}{2}\right]^T \tag{4.10}$$

Numerical Quadrature

Using the trapezium rule over each element,

$$\int_{x_{i-1}}^{x_i} f(x)dx \approx \frac{f(x_i)+f(x_{i-1})}{2}\cdot h_{i-1}, \quad 2 \le i \le N+1, \tag{4.11}$$

for the numerical evaluation of the integrals which appear in (4.7)-(4.8), the nonlinear IVP (4.5)-(4.6) can be simplified.

Denoting the matrices resulting from this numerical quadrature as $\tilde{M}$, $\tilde{Q}$, ..., one has

$$\tilde{M} = \text{diag}\left(\frac{h_1}{2}, \frac{h_1+h_2}{2}, \ldots, \frac{h_{i-1}+h_i}{2}, \ldots, \frac{h_{N-1}+h_N}{2}\right),$$

$$\tilde{Q} = Q, \quad \tilde{E} = E,$$

$$\tilde{R} = -\left[\frac{x_i}{2}, 0, \frac{x_i}{2}\right]_{1\le i\le N},$$

$$\tilde{P} = [\tilde{p}_1, \tilde{p}_2, \ldots, \tilde{p}_N]^T, \tag{4.12}$$

with

$$\tilde{p}_i = \frac{h_{i-1}+h_i}{2} \cdot [(L\cdot(1-x_i)+R_0\cdot x_i)\cdot c_0(L\cdot(1-x_i)+R_0\cdot x_i) - c_I\cdot R_0],$$
$$1 \le i \le N, \quad (h_0 = 0).$$

Notice that the diagonal matrix $\tilde{M}$ turns out to be the lumped matrix of the original mass matrix M, as it should.

The IVP (4.5)-(4.6) or the related simplified IVP, which results from the use of the numerical quadrature (4.11), can be solved numerically by well established time discretization techniques. We have chosen a step-controlled Runge Kutta scheme, available e.g. from Mathematica 2.2.

5 NUMERICAL RESULTS

5.1 Precipitate growth

For the case of precipitate growth we may compare the results obtained by the numerical method described above with the exact solution which was derived in Aaron et *al.* [3], for the *special data* $L = \infty$, $R_0 = 0$ and $c_0 = c_M$ = constant. In our model we take $L = 10$, and we impose the homogeneous Neumann BC, $\partial_r c = 0$, at $r = L$, corresponding to the limit condition $c(+\infty, t) = c_M$ considered in [3]. Moreover we choose $R_0 \approx 10^{-4}, 10^{-3}$ and 10^{-2}, the system (4.5)-(4.6) being singular when $R_0 = 0$.

We should find that during a *short* time interval $[0, t_e]$, the length of which depends on the kinetics parameter, used in [3], viz

$$k = 2\cdot\frac{c_M - c_I}{c_P - c_I}, \tag{5.1}$$

the numerical results are in good agreement with the exact ones from [3], as for small values of t the influence of the finite matrix boundary on the precipitate growth is negligible.

At the other hand, for large values of time the radius $R(t)$ of the precipitate should tend to the value R_∞, corresponding to the steady state regime and being obtainable from a conservation of mass argument in the precipitate and the matrix. This mass balance reads

$$L^3 \cdot c_M = R_\infty^3 \cdot c_p + (L^3 - R_\infty^3) \cdot c_I \tag{5.2}$$

as in the steady state regime the concentration of dissolved element in the matrix is $c = c_I$ throughout.

By numerous numerical experiments, summarized in the tables below, we analyze the following *3 aspects*

1. The dependence of the procentual errors

$$\varepsilon = \max_{[a,b]} \frac{|R_N(t) - R_e(t)|}{R_e(t)} \cdot 100, \quad \tilde{\varepsilon} = \max_{[a,b]} \frac{|\tilde{R}_N(t) - R_e(t)|}{R_e(t)} \cdot 100, \quad (5.3) - (5.4)$$

on the number of the elements N. See Tables I and II. Cf. also Figures 4, 5 and 6.

Here $R_e(t)$ is the precipitate radius at time t derived from the exact solution in [3], while $R_N(t)$ and $\tilde{R}_N(t)$ are the approximate values of this radius obtained by the method outlined in Section 4, without or with use of numerical quadrature, respectively.

2. The influence of the choice of (a small value of) R_0 on the error $\in$, (5.3), for different values of N. See Table I.

3. The dependence of the error ε, (5.3), and of the time $\bar{T}_\infty$ on the kinetics parameter k, (5.1), for $N = 10$. See Table III. Here $\bar{T}_\infty$ is the time (estimated from below) such that

$$\left| \frac{R_\infty}{R_N(t)} - 1 \right| < 10^{-4} \quad \text{for} \quad t > \bar{T}_\infty \tag{5.5}$$

The time interval $[a, b]$ in the definition (5.3)-(5.4) is chosen so that the influence of the finite matrix cell radius on the approximate precipitate radius $R_N(t)$ is negligible.

In all experiments the *data* are: $L = 10$; $D = 1$ and, apart from Table III, $c_I = 1, c_M = 2$, $c_P = 6.062$, $(k = 0.3951)$.

TABLE I Precipitate growth. The error ε, (5.3), for different values of R_0 and N.

R0\ N	*4*		*7*		*10*		*20*	
10^{-2}	6	3	1	0.4	0.4	0.35	0.4	0.4
10^{-3}	5	1	1	0.35	0.35	0.35	0.35	0.4
10^{-4}	20	1	1	0.35	0.4	0.4	0.3	0.4

In each 1st subcolumn ε corresponds to the time interval [0.5, 5], in each 2nd subcolumn ε is related to the time interval [5, 20].

TABLE II Precipitate growth. The errors ε, (5.3), and $\tilde{\varepsilon}$, (5.4), for different values of N, when $R_0 = 10^{-3}$

N	*4*		*7*		*10*		*20*	
ε	5	1	1	0.35	0.4	0.4	1	0.9
$\tilde{\epsilon}$	14	1.5	1.2	1	1.2	0.9	0.4	0.4

In each 1st subcolumn ε and $\tilde{\varepsilon}$ correspond to the time interval [0.5,5], in each 2nd subcolumn they are related to the time interval [5,20].

TABLE III Precipitate growth. Dependence of the error ε, (5.3), and of the time $\overline{T}_\infty$, (5.5), on the kinetics parameter k, (5.1), when $N = 10$ and $R_0 = 10^{-3}$

k	$6.173 \cdot 10^{-7}$	$3.086 \cdot 10^{-4}$	$6.17 \cdot 10^{-3}$	*0.02469*	*0.06173*
ε	3	0.8	0.5	0.3	0.3
$\overline{T}_\infty$	3000	8000	1500	1000	800
(a,b)	(0.5,40)				

k	*0.2716*	*0.3951*	*0.5802*	*1.5*
ε	0.4	0.3	0.4	0.5
$\overline{T}_\infty$	150	100	50	50
(a, b)	(0.5, 25)	(0.5, 20)	(0.5, 18)	(0.5, 5)

The error ε is evaluated over the respective time intervals indicated on the bottom line.

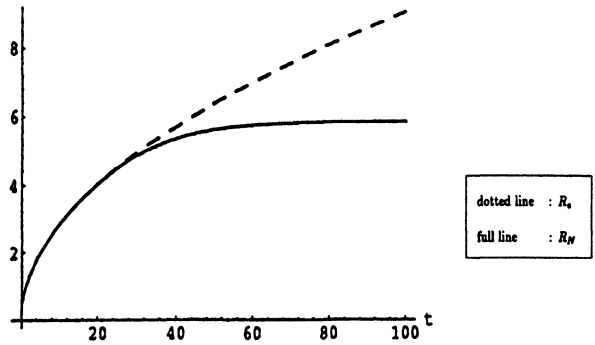

FIGURE 4 Precipitate growth. R_N and R_e versus time when $N = 7$ and $R_0 = 10^{-3}$

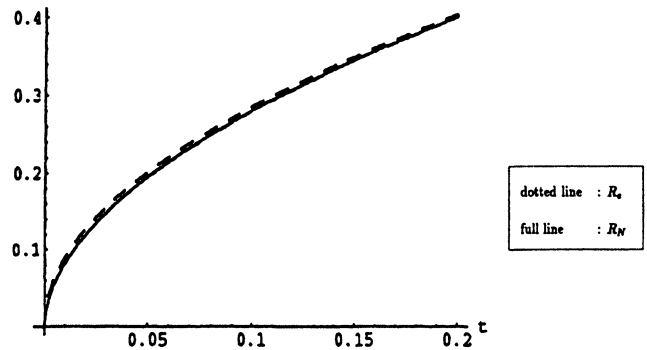

FIGURE 5 Precipitate growth. R_N and R_e versus time in the interval [0, 0.2] when $N = 7$ and $R_0 = 10^{-3}$

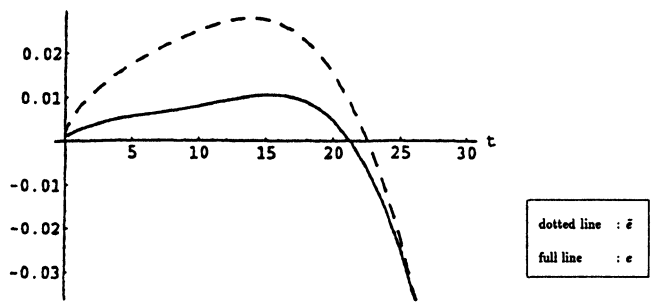

FIGURE 6 Precipitate growth. Time evolution of the errors $e = R_N - R_e$ and $\tilde{e} = \tilde{R}_N - R_e$ when $N = 10$ and $R_0 = 10^{-3}$

5.2 Precipitate dissolution

For precipitate dissolution there is no exact solution available to the FBP (2.1)-(2.5) for a particular choice of the data, even not for the idealized case that $L = \infty$. However, when the precipitate gets not dissolved completely, the method outlined in Section 4 can still be tested by means of the precipitate radius $R_N(t)$ for large values of time. Indeed, this radius should again tend to the value R_∞, corresponding to the steady state regime and being given by the mass balance argument (conservation of initial mass), which now reads

$$R_0^3 \cdot c_P + (L^3 - R_0^3) \cdot c_M = R_\infty^3 \cdot c_P + (L^3 - R_\infty^3) \cdot c_I$$

The numerical experiments for $R_N(t)$ at $t = 500$, shown in Table 4, are in agreement with this observation, see also Fig. 7. Both for Table IV and Fig. 7, the *data* are: $L = 10$, $R_0 = 5$; $c_I = 1$, $c_M = 0.84$, $c_p = 3$ $(k = -0.16)$; $D = 1$. A similar precision has been obtained for a large scale of the kinetics parameter k.

TABLE IV Precipitate dissolution up to steady state regime ($R_\infty = 3.80295$). Value of $1 - \frac{R_N(500)}{R_\infty}$ for different values of N, without and with use of numerical quadrature

N	4	7	10	20
exact quadrature	0.00159	0.00030	0.00012	0.00012
numerical quadrature	0.00685	0.00214	0.00105	0.00027

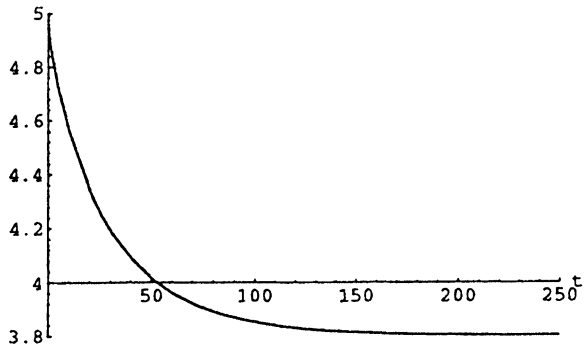

FIGURE 7 Precipitate dissolution. Time evolution of the precipitate radius R_{10} up to steady state regime. ($R_\infty = 3.80295$)

When, for a fixed value of the kinetics parameter k, the ratio $\frac{R_0}{L}$ of the initial radius of the particle and of the matrix cell radius L is taken to be sufficiently small, the particle should be dissolved completely after a finite time T_e. This finite extinction time phenomenon has been confirmed properly by the numerical experiments, such as those summarized in Fig. 8 and Table V below.

In Fig. 8 we compare the time evolution of the precipitate radius, calculated by the present method (again for $N = 10$), with the one shown in Aaron *et al.* [3], for the indicated set of data (apart from the choice $L = \infty$ in that paper). The result from [3] is based on a stationary interface approximation method. As in our numerical $\frac{R_0}{L} = 0.05$, the influence of the finite matrix cell boundary on the dissolution process is negligible. Hence, a comparison of both extinction times is meaningful. From Fig. 8 their difference is seen to be about 8.5 %.

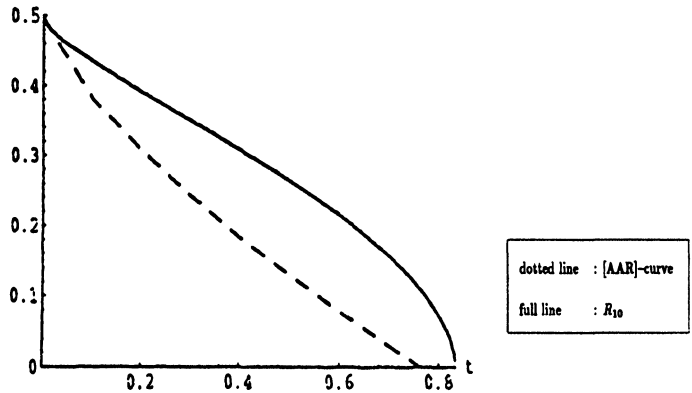

FIGURE 8 Precipitate dissolution up to complete extinction. Time evolution of the precipitate radius R_{10}. Comparison with [3]. Case: $L = 10$, $R_0 = 0.5$; $c_I = 2$, $c_M = 1$, $c_p = 10$ ($k = -0.25$); $D = 1$

Table V shows the expected dependence of the extinction time T_e on the kinetics parameter k, (5.1), (through the interface concentration c_I). Notice that the value of T_e is nearly affected by the use of numerical quadrature. Moreover, for a fixed c_I, T_e is found to retain its value when L is further increased, as it should, because the influence of the matrix cell boundary on the dissolution process is negligible from a sufficiently small ratio $\frac{R_0}{L}$

on. *Small* variations in the value of T_e (for a fixed c_I) when successively L = 10, 30 and 50, can be expected a priori: as a fixed number of elements in the mesh (N = 10) is retained , in particular the density of the grid points near the point x = 1, that corresponds to the matrix-precipitate interface, decreases for increasing L.

The calculations are done for a set of data corresponding to a set in Asthana and Pabi [1], (although the ratio $\frac{R_0}{L}$ is not mentioned in that paper). The respective values of T_e for c_I = 0.06 deviate at most 5 % from the value T_e = 6.404, obtained in [1] by means of Whelan's stationary interface model [7].

TABLE V Precipitate dissolution up to complete extinction.. Extinction time T_e for different values of c_I, calculated with N = 10. Case: R_0 = 1; c_M = 0, c_p = 1; D = 1

$c_I \setminus L$	*10*		*30*		*50*	
0.06	6.741	6.723	6.597	6.722	6.655	6.720
0.07	5.671	5.655	5.531	5.655	5.598	5.653
0.10	3.772	3.762	3.642	3.761	3.726	3.761
0.30	0.963	0.962	0.865	0.961	0.930	0.960

Each 1st subcolumn gives the value of T_e obtained with exact quadrature, each 2nd subcolumn gives the corresponding value obtained with numerical quadrature.

Finally, the computed curve in Fig. 8 is convex-concave, reflecting the expected time evolution of the interface velocity $\frac{dR}{dt}$ in the case of complete precipitate dissolution.

5.3 Discussion

The numerical results presented above support the reliability of the approximation method described in Sections 3–4. The most striking points are the following ones:

- Good numerical results are already obtained with a coarse finite element mesh, viz N = 10 or even N = 7, cf. Table I [even for N = 4 the

numerical results are quite satisfactory for not too small values of time] and cf. Table IV.

- The use of a simple numerical quadrature rule for the construction of the finite element matrices, implying a considerable simplification of the IVP (4.5)-(4.6), doesn't deteriate the numerical results, cf. Table II, Table IV and Table V.
- The choices $R_0 = 10^{-2}, 10^{-3}$ and 10^{-4} for the initial precipitate radius in the case of precipitate growth don't influence much the numerical results, [except for a coarse mesh when $R_0 = 10^{-4}$], cf. Table I.
- The precision of the numerical results remains high for a large scale of the kinetics parameter k, cf. Table III .

6 CONCLUDING REMARKS AND FUTURE DIRECTIONS

This paper dealt with a mathematical model of the diffusion-controlled growth and dissolution of spherical precipitates in a spherical, homogeneous matrix. We presented a numerical approximation method for the underlying FBP (2.1)-(2.5). That method basically rests upon (1) a fixed domain transformation, (2) a nonconforming finite element method, moreover with a nonuniform linear mesh and a suitable flux approximation technique, applied to the resulting highly nonlinear and nonlocal parabolic problem. Numerical experiments have confirmed the method to be effective and reliable. In fact, even a numerical quadrature FE-method on a coarse mesh provides adequate results. As moreover the time discretization of the resulting IVP for a system of strongly nonlinear 1st order ODEs has been done with a well established, step-controlled Runge Kutta code, the complete numerical scheme can be implemented on PC.

The work reported on in this paper can be extended in a few directions. First, the numerical approximation method outlined above can be adapted so as to cope with non constant data, in particular with a concentration dependent diffusion coefficient. Secondly, in a physically more elaborated model, the dissolution/growth process must not be assumed to take place at a constant homogeneous temperature. In fact, that process is related to the time variation of the temperature in the spherical cell (through the temperature varying diffusion coefficient and interface concentration). Thus a coupled parabolic problem for $[R, c]$ and T (temperature field) can be stud-

ied. Thirdly, the basic ideas (1)-(2) summarized above can also serve as the starting point for the numerical analysis of some other types of diffusion processes with moving boundaries, for instance arising from chemical kinetics, see e.g. Chapter 6 in Froment and Bisschoff [8]. In particular, we mention a transient 2-component diffusion problem in 1D, arising from the kinetic modelling of the adsorption process of dilute SO_2 in aqueous Na_2SO_3 solutes, see De Smul [9]. This problem is a topic of ongoing research.

Acknowledgements

We thank the Belgian National Foundation for Scientific Research (NFWO) for financial support. We thank G. CAERS and Y. HOUBAERT of the Laboratory of Metallurgy and Material Science of the University of Ghent (Belgium) for bringing us into contact with the topic of this paper. We are grateful to Dr. J. POUSIN of The National Institute of Applied Sciences (INSA) in Lyon (France) for his critical comments on a former version of this paper.

References

[1] R. Asthana and S.K. Pabi, An Approximate Solution for the Finite-extent Moving-boundary Diffusion-controlled Dissolution of Spheres, *Mater.* Sci. *Eng. A.,* **128** (1990), pp. 253–257.

[2] G. Caers, *Mathematical model for dissolution and precipitation of AlN* in *steel,* (in Dutch), Thesis, Laboratory of Metallurgy and Material Science, University of Ghent, Belgium (1992).

[3] H.B. Aaron, D. Fainstein and G.R. Kotler, Diffusion-Limited Phase Transformations: A Comparison and Critical Evaluation of the Mathematical Approximations, *J. Appl. Phys.,* **41** (1970), pp. 4404–4410.

[4] W.J. Liu, E.B. Hawbolt and I.V. Samarasekra, Finite difference modelling of the growth and dissolution of carbonitride precipitates in austinite. In: S. Yue, (Ed.), *Proceedings of the international symposium on the mathematical modelling of hot rolling of steel,* Publ. Canadian Institute of Minig and Metallurgy, Hamilton, Canada, 1990, pp. 477–487.

[5] A.K. Pani, A finite element approximation to the unidimensional nonlinear ablation problem. In: R.W. Lewis and K. Morgan (Eds.), *Numerical Methods in Thermal Problems VI*, Pineridge Press, Swansea, 1989, pp. 101-l10.

[6] G.F. Carey and J.T. Oden, *Finite Elements II,* Prentice-Hall, Inc., Englewood Cliffs, New Jersey, 1983, pp. 254–268.

[7] M.J. Whelan, On the Kinetics of Precipitate Dissolution, *Metal Sc. J.*, **3** (1969), pp. 95–97.

[8] G.F. Froment and K.B. Bisschoff, *Chemical Reactor Analysis and Design,* J. Wiley, New York, 1991, pp. 205–344.

[9] A. De Smul, *Kinetic modelling of the absorption of SO_2 in aqueous $NaSO_3$-solutes,* (in Dutch), Thesis, Department of Technical Chemistry and Environmental Technology, University of Ghent, Belgium (1994).

Mathematical Problems in Engineering

Special Issue on
Modeling Experimental Nonlinear Dynamics and Chaotic Scenarios

Call for Papers

Thinking about nonlinearity in engineering areas, up to the 70s, was focused on intentionally built nonlinear parts in order to improve the operational characteristics of a device or system. Keying, saturation, hysteretic phenomena, and dead zones were added to existing devices increasing their behavior diversity and precision. In this context, an intrinsic nonlinearity was treated just as a linear approximation, around equilibrium points.

Inspired on the rediscovering of the richness of nonlinear and chaotic phenomena, engineers started using analytical tools from "Qualitative Theory of Differential Equations," allowing more precise analysis and synthesis, in order to produce new vital products and services. Bifurcation theory, dynamical systems and chaos started to be part of the mandatory set of tools for design engineers.

This proposed special edition of the *Mathematical Problems in Engineering* aims to provide a picture of the importance of the bifurcation theory, relating it with nonlinear and chaotic dynamics for natural and engineered systems. Ideas of how this dynamics can be captured through precisely tailored real and numerical experiments and understanding by the combination of specific tools that associate dynamical system theory and geometric tools in a very clever, sophisticated, and at the same time simple and unique analytical environment are the subject of this issue, allowing new methods to design high-precision devices and equipment.

Authors should follow the Mathematical Problems in Engineering manuscript format described at http://www.hindawi.com/journals/mpe/. Prospective authors should submit an electronic copy of their complete manuscript through the journal Manuscript Tracking System at http://mts.hindawi.com/ according to the following timetable:

Manuscript Due	February 1, 2009
First Round of Reviews	May 1, 2009
Publication Date	August 1, 2009

Guest Editors

José Roberto Castilho Piqueira, Telecommunication and Control Engineering Department, Polytechnic School, The University of São Paulo, 05508-970 São Paulo, Brazil; piqueira@lac.usp.br

Elbert E. Neher Macau, Laboratório Associado de Matemática Aplicada e Computação (LAC), Instituto Nacional de Pesquisas Espaciais (INPE), São Josè dos Campos, 12227-010 São Paulo, Brazil ; elbert@lac.inpe.br

Celso Grebogi, Department of Physics, King's College, University of Aberdeen, Aberdeen AB24 3UE, UK; grebogi@abdn.ac.uk